Archival Report

Biological Psychiatry: GOS

Associations Between Brain Structural Alterations, Executive Dysfunction, and General Psychopathology in a Healthy and Cross-Diagnostic Adult Patient Sample

Adrienne L. Romer and Diego A. Pizzagalli

ABSTRACT

BACKGROUND: A general psychopathology factor (p factor) captures shared variance across mental disorders in diverse samples and may partly reflect executive dysfunction. Higher p factor scores have been related to structural alterations within the visual association cortex (VAC) and a cerebello-thalamo-cerebro-cortical circuit, both of which are important for executive control. Here, we tested replicability of these direct associations as well as the indirect role of executive functioning in a sample of healthy and cross-diagnostic adult patients.

METHODS: We conducted hypothesis-driven (i.e., region of interest) and exploratory whole-brain structural neuroimaging analyses using data from the Consortium for Neuropsychiatric Phenomics (CNP) study of 272 adults who met diagnostic criteria for schizophrenia, bipolar disorder, or attention-deficit/hyperactivity disorder or were healthy control subjects. Using structural equation modeling, we examined direct and indirect relations between structural neural alterations (within regions of interest and regions identified from exploratory analyses) and p and executive function factors.

RESULTS: Higher levels of the p factor were associated with decreased executive functioning and VAC gray matter volume, replicating previous research. In contrast, we failed to replicate previous negative relations between the p factor and cerebello-thalamo-cerebro-cortical circuit structure. A significant indirect relation between VAC gray matter volume and the p factor via executive function also emerged. Whole-brain analyses identified additional structural alterations in supplementary motor area/cingulate cortex, anterior corona radiata, and corpus callosum genu related to the p factor.

CONCLUSIONS: Executive dysfunction may be one mechanism underlying relations between brain structure and general psychopathology. Replication of VAC structural alterations related to the p factor encourages further focus on this brain structure.

https://doi.org/10.1016/j.bpsgos.2021.06.002

High rates of comorbidity (~50%) (1) have encouraged a shift in focus toward transdiagnostic models of psychopathology. In support of this shift, factor-analytic models have identified a general psychopathology factor (p factor) capturing shared variation in internalizing, externalizing, and thought disorders in diverse samples over the life span (2–4). The meaning of the p factor is not yet clear, although multiple theories have been proposed (2). One conceptualization of the p factor is that it may partly reflect executive dysfunctions present not only in thought disorders but also in extreme presentations of internalizing and externalizing disorders. Indeed, poor executive function (EF) has been posited as a transdiagnostic cognitive dysfunction linked to psychiatric disorders (5–8) and, specifically, negatively related to the p factor (9–17).

Recent structural neuroimaging research has identified neural abnormalities associated with the p factor that may subserve EF, including within the visual association cortex (VAC) and a cerebello-thalamo-cerebro-cortical circuit (CTCC) (18–20). This research found reduced gray matter volume (GMV) of the VAC and posterior cerebellum and lower fractional anisotropy (FA) of the pons related to higher p factor scores (18). The pons mediates communication between the prefrontal cortex and posterior cerebellum as part of this CTCC (21,22). In addition to these specific structural neural alterations, other studies have identified global patterns of reduced GMV (23,24) and neocortical thickness (25) related to a higher p factor.

Although not usually considered as key EF regions, the VAC and CTCC are implicated in executive control through their connections with the prefrontal cortex and are activated during EF tasks (26–32). The VAC is involved in the selection and suppression of task-relevant versus task-irrelevant visual information (26,27). High p factor scores have also been associated with inefficient intrinsic functional connectivity between the VAC and frontoparietal and default mode networks that support executive control and self-referential processes,

SEE COMMENTARY ON PAGE 2

ISSN: 2667-1743

respectively (33). The CTCC is thought to function as a forward controller, comparing intention with the execution of behaviors by continuously updating internal models (34,35). CTCC dysfunction has been reported consistently in disorders characterized by poor EF and disorganized thought (i.e., schizophrenia) (36–38). Moreover, individuals with cerebellar cognitive affective syndrome following damage to the posterior cerebellum experience executive dysfunction referred to as dysmetria of thought (39–41).

However, little research has directly linked these structural alterations associated with the p factor to EF performance. Further, the hypothesis that individual differences in EF might explain such relations between brain structure and the p factor has not yet been tested. In this study, we assessed the relationships between brain structural alterations previously associated with variation in the p factor and neurocognitive measures of EF and tested an indirect path from brain structure to the p factor via EF. In addition, whereas many studies have included community/volunteer samples, we examined these relationships in an adult case-control sample.

We used psychiatric symptom, neurocognitive, and multimodal structural magnetic resonance imaging (MRI) data from the Consortium for Neuropsychiatric Phenomics (CNP) sample of 272 adults aged 21–50 years. The sample includes 130 adults without any DSM-IV diagnosis (i.e., healthy control subjects) and 142 patients with schizophrenia, bipolar I, or attention-deficit/hyperactivity disorder (ADHD) diagnoses. Instead of pursuing a case-control approach, we used psychiatric symptom data to identify a p factor across all four groups. We conducted hypothesis-driven, region-of-interest (ROI) analyses of VAC and CTCC structure (i.e., posterior cerebellum and pons). In addition, we conducted whole-brain exploratory analyses of GMV and FA to determine whether alterations in brain regions not previously hypothesized also may be related to the p factor in this sample. We then used structural equation modeling (SEM) to test direct and indirect paths from brain structure to the p factor via EF.

For the ROI analyses, we tested the following hypotheses: 1) poor EF would be associated with higher levels of the p factor; 2) reduced VAC and cerebellar GMV and poorer pons FA would be associated with higher levels of the p factor; and 3) there would be a significant indirect relation between these structural neural alterations and the p factor via EF. As other studies have identified global brain structural alterations related to p (20–22), we also examined relations between the p factor and global GMV, cortical thickness (CT), and surface area (SA). Finally, we determined whether relations between brain structure, EF, and psychopathology were unique to psychopathology dimensions (internalizing, externalizing, thought) or EF components (working memory, shifting, inhibition) beyond their relations with general p and EF factors.

METHODS AND MATERIALS

Full details on methods and materials are presented in the Supplement.

Participants

We downloaded the University of California, Los Angeles, CNP dataset (42) from the public database OpenNeuro (https://openneuro.org/datasets/ds000030) (43), comprising psychiatric symptom, neurocognitive, and multimodal neuroimaging data from 272 participants, including 130 healthy control individuals, 50 patients with schizophrenia or schizoaffective disorder, 49 patients with bipolar I disorder, and 43 patients with ADHD. Notably, 81% of patients had at least one comorbid mental disorder.

Details about participant recruitment are reported elsewhere (42). Briefly, healthy adults were recruited from the Los Angeles area via community advertisements. Patients were recruited via local clinics and online portals. Inclusion criteria were ages 21–50, either White (not Hispanic/Latino) or Hispanic/Latino (of any race), primary language either English or Spanish, ≥8 years of formal education, and no significant medical illness. Participants were screened for cannabis, amphetamine, opioids, cocaine, and benzodiazepines and were excluded if urinalysis results were positive. Other exclusion criteria were being left-handed, pregnancy, history of head injury with loss of consciousness or cognitive sequelae, or other MRI contraindications (e.g., claustrophobia). Each patient group excluded anyone with one of these other diagnoses (e.g., schizophrenia could not meet ADHD diagnostic criteria). Stable medications were permitted for patients (73% reported lifetime psychotropic medication use) (Table S1). Participants provided written informed consent following procedures approved by the Institutional Review Boards at University of California Los Angeles and the Los Angeles County Department of Mental Health. Participants with missing T1w (n = 7) or diffusion data (n = 14) were excluded from analyses (GMV inclusion n = 265; FA inclusion n = 258).

Psychiatric Symptoms

Participants completed the Structured Clinical Interview for DSM-IV-Text Revision (44) and a battery of mental health questionnaires. Twelve symptoms were measured: depression, anxiety, somatization, interpersonal sensitivity, ADHD, impulsivity, alcohol, cannabis, other substance use, obsessive-compulsive disorder, mania, and schizophrenia.

Executive Function

Participants completed a battery of neurocognitive tests measuring different EF components (45). A total of 15 performance scores from 13 neurocognitive tests were used to tap working memory (WM), shifting, and inhibition EF components.

MRI Acquisition and Processing

MRI data were acquired on one of two 3T Siemens Trio scanners at the Ahmanson-Lovelace Brain Mapping Center (Siemens version syngo MR B15) and the Staglin Center for Cognitive Neuroscience (Siemens version syngo MR B17) at University of California Los Angeles. High-resolution magnetization-prepared rapid acquisition gradient-echo anatomical scans were collected using the following sequence: repetition time = 1.9 seconds, echo time = 2.26 ms, field of view = 250 mm, matrix = 256 × 256, sagittal plane, slice thickness = 1 mm, 176 slices. Diffusion-weighted imaging data were collected using an echo-planar sequence with parameters: 64 directions, 2-mm slices, repetition time/echo

time = 9000/93 ms, 1 average, 96 × 96 matrix, 90° flip angle, axial slices, b = 1000 s/mm^2.

All image processing followed procedures from Romer *et al.* (18,19). Regional GMVs were determined using the unified segmentation (46) and DARTEL normalization (47) in SPM12 implemented in MATLAB (R2019a; The MathWorks, Inc.). Individual T1-weighted images were segmented into gray, white, and cerebrospinal fluid images and then nonlinearly registered to the existing Information eXtraction from Images template of 550 healthy subjects averaged in standard Montreal Neurological Institute space, available with VBM8. GM images were modulated for nonlinear effects of the high-dimensional normalization to preserve the total amount of signal from each region and smoothed with an 8-mm full width at half maximum Gaussian kernel (1.5 × 1.5 × 1.5 mm voxel size). A GM mask was created by thresholding the final stage (6th) Information eXtraction from Images template at 0.1.

The Spatially Unbiased Infratentorial Toolbox (SUIT) (48) was used for high-resolution cerebellar-specific voxel-based morphometry (VBM) analyses. The toolbox's Isolate function was used to create a mask of the cerebellum and generate gray and white matter segmentation maps. The masked segmentation maps were normalized to the SUIT template with nonlinear DARTEL normalization. The resulting cerebellar GM image was resliced into the SUIT atlas space and smoothed with a 4-mm full width at half maximum isotropic Gaussian kernel.

Diffusion tensor imaging (DTI) analyses were completed using SPM8. All diffusion-weighted scans were motion-corrected and coregistered to the mean image to correct for head movement. The tensor model was used to calculate FA

Table 1. Descriptive Statistics of Study Variables for the Overall Sample and for Each Diagnostic Group

	Overall, N = 265	HC, n = 125	ADHD, n = 41	BD, n = 49	SZ, n = 50	F/χ^2 (df)	p Value
Covariates							
Age, Mean (SD)	33.23 (9.30)	31.53 (8.80)	32.34 (10.45)	35.29 (9.03)	36.46 (8.88)	4.49 (3)	.004[a]
Gender, Women, n (%)	112 (42.3%)	59 (47.2%)	20 (48.8%)	21 (42.9%)	12 (24.0%)	8.80 (3)	.032
Race, n (%)						41.25 (15)	<.001[a]
AA	6 (2.3%)	1 (0.8%)	1 (2.4%)	1 (2.0%)	3 (6.0%)		
AI/AN	40 (15.1%)	25 (20.0%)	0 (0.0%)	4 (8.2%)	11 (22.0%)		
Asian	4 (1.5%)	2 (1.6%)	1 (2.4%)	0 (0%)	1 (2.0%)		
Multiracial	11 (4.2%)	0 (0.0%)	3 (7.3%)	7 (14.3%)	1 (2.0%)		
White	203 (76.6%)	97 (77.6%)	36 (87.8%)	37 (75.5%)	33 (66.0%)		
Ethnicity, Hispanic, n (%)	93 (35.1%)	45 (36.0%)	6 (14.6%)	13 (26.5%)	29 (58.0%)	20.68 (3)	<.001[a]
Site 1, n (%)	174 (65.7%)	102 (81.6%)	21 (51.2%)	26 (53.1%)	25 (50.0%)	26.77 (3)	<.001[a]
ICV, Mean (SD)	1,530,915.73 (179,937.71)	1,521,587.27 (194,121.31)	1,566,172.94 (166,384.20)	1,526,135.87 (180,243.54)	1,529,991.77 (152,263.31)	0.646 (3)	.586
Average FA, Mean (SD)	0.40 (0.02)	0.40 (0.01)	0.40 (0.01)	0.40 (0.03)	0.40 (0.01)	3.48 (3)	.017[a]
Factor Scores							
p Factor, Mean (SD)	100.00 (15.00)	90.35 (6.30)	101.07 (9.68)	112.54 (15.78)	110.97 (16.51)	65.09 (3)	<.001[a]
EF Factor, Mean (SD)	100.00 (15.00)	106.27 (12.34)	100.86 (12.33)	98.69 (13.50)	84.89 (13.72)	33.32 (3)	<.001[a]
ROIs							
VAC GMV, Mean (SD)	0.53 (0.06)	0.54 (0.06)	0.53 (0.07)	0.53 (0.06)	0.50 (0.05)	6.26 (3)	<.001[a]
Posterior Cerebellar GMV, Mean (SD)	0.65 (0.08)	0.66 (0.08)	0.66 (0.08)	0.67 (0.07)	0.63 (0.06)	2.65 (3)	.049
Lobule VIIB GMV, Mean (SD)	0.81 (0.09)	0.81 (0.08)	0.85 (0.09)	0.81 (0.09)	0.77 (0.09)	5.66 (3)	.001[a]
Pons FA, Mean (SD)[b]	0.48 (0.03)	0.48 (0.04)	0.47 (0.03)	0.48 (0.03)	0.47 (0.03)	2.32 (3)	.076
Global Structure							
Total GMV, Mean (SD)	648,309.67 (63,692.26)	654,306.37 (64,235.81)	654,661.14 (60,458.63)	646,703.55 (66,810.76)	629,303.57 (59,654.81)	1.99 (3)	.116
Average CT, Mean (SD)	2.47 (0.08)	2.48 (0.08)	2.50 (0.08)	2.45 (0.08)	2.44 (0.09)	5.82 (3)	.001[a]
Total SA, Mean (SD)	175,555.90 (17,473.48)	177,213.34 (17,749.01)	173,491.19 (18,642.58)	176,102.50 (17,642.31)	172,508.73 (15,415.62)	1.08 (3)	.358

Groups were compared with either analyses of variance (for continuous measures) or χ^2 tests (for categorical measures). One participant did not report their race. p Values are unadjusted.

AA, African American; ADHD, attention-deficit/hyperactivity disorder; AI/AN, American Indian/Alaskan Native; BD, bipolar disorder; CT, cortical thickness; EF, executive function; FA, fractional anisotropy; GMV, gray matter volume; HC, healthy control; ICV, intracranial volume; ROIs, regions of interest; SA, surface area; SZ, schizophrenia; VAC, visual association cortex.

[a]p values that survived false discovery rate correction for the 16 tests ($q < .05$).

[b]Descriptive statistics are reported for the 223 participants with adequate pons coverage (HC: n = 96; SZ: n = 46; BD: n = 44; ADHD: n = 37).

values for each voxel, and nonbrain tissue was removed. Each image was normalized to Montreal Neurological Institute space and smoothed using a 4-mm full width at half maximum Gaussian kernel. Images were visually inspected for quality.

Regions-of-Interest and Global Structure Measures

Exact masks were created from the four primary associations with the p factor originally reported in Romer *et al.* (18): 137-voxel pons cluster, 2353-voxel VAC cluster, 709-voxel posterior cerebellum cluster, and 156-voxel cerebellar lobule VIIB cluster (Figure S1). Mean values for these masks were extracted for each participant from the FA (pons), GMV (VAC and cerebellum), and SUIT maps (lobule VIIB). After visual inspection, 34 participants' FA maps demonstrated poor coverage of the pons ROI and were removed from analyses of pons FA. One additional participant was excluded because their estimated FA was >3 SDs from the mean (n = 223). We also extracted total GMV, average CT, and total SA estimates using the recon-all processing pipeline (49) from FreeSurfer (version 6.0.011) (50).

Statistical Analyses

Analyses were conducted in the following steps. First, we used confirmatory factor analysis (CFA) to fit measurement models of psychopathology and EF. Second, we conducted whole-brain exploratory analyses of GMV and FA related to p factor scores extracted from the CFA. Third, we used SEM to identify direct and indirect relations between brain structure and p and EF factors.

Confirmatory Factor Analyses

Measurement models of psychopathology and EF were fit (see Tables S2 and S3 for symptoms and neurocognitive test intercorrelations). For the CFA of psychopathology, a higher-order model was tested in which the symptom measures loaded on their respective lower-order internalizing, externalizing, and thought disorder factors, each of which loaded on a general p factor. We opted for a higher-order over a bifactor model owing to concerns about overfitting (51); moreover, this higher-order structure is consistent with the Hierarchical Taxonomy of Psychopathology model (52). Based on previous research that the 15 neurocognitive tests measured WM, shifting, and inhibition constructs (45), a higher-order CFA was fit in which the tests loaded on their respective lower-order WM, shifting, and inhibition factors, each of which loaded on a general EF factor. Correlated factors models also were tested, which are equivalent to higher-order models without including a general factor. Measurement model estimates were fixed in subsequent SEM analyses.

Exploratory Analyses

Whole-brain analyses of GMV and FA were conducted in SPM12 using VBM and DTI, respectively. p Factor scores were extracted from the CFA using the standard regression method and were standardized (mean = 100, SD = 15). Multiple linear regressions were conducted with p factor scores predicting differences in GMV and FA controlling for gender, age, race/ethnicity, site, and total intracranial volume for VBM and average whole-brain FA values for DTI analyses, using Monte Carlo simulation-derived whole-brain corrected thresholds. Estimates of significant clusters were extracted for further SEM analysis.

SEM Analyses

We tested SEMs whereby the p and EF factors were regressed on the ROIs (VAC, posterior cerebellum, cerebellar lobule VIIB,

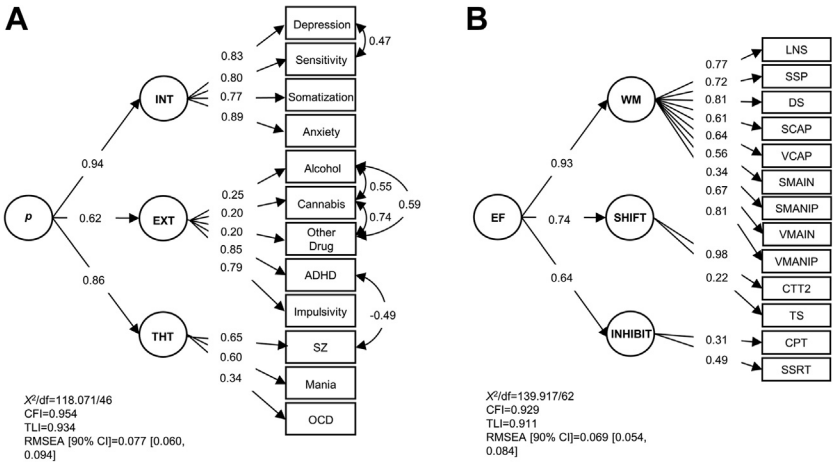

Figure 1. Confirmatory factor analysis models of the structure of psychopathology and executive function. Confirmatory factor analyses are depicted for the higher-order structure of psychopathology **(A)** and executive function (EF) **(B)**. Model fit statistics and standardized loadings are reported. **(A)** The 12 symptom measures load on the lower-order internalizing (INT), externalizing (EXT), and thought disorder (THT) factors, which subsequently load on a general p factor. **(B)** The 13 EF tests load on the lower-order working memory (WM), shifting (SHIFT), and inhibition (INHIBIT) factors, which subsequently load on a general EF factor. Depression was assessed with Hopkins Symptom Checklist (HSCL) Depression subscale; sensitivity was assessed with HSCL Interpersonal Sensitivity subscale; somatization was assessed with the HSCL Somatization subscale; anxiety was assessed with the HSCL Anxiety subscale; ADHD symptoms were assessed with the Adult Self-Report Scale V.1.1 Screener; impulsivity was assessed with the Barratt Impulsiveness Scale-Brief; all other symptoms were assessed with the SCID. ADHD, attention-deficit/hyperactivity disorder; alcohol, alcohol use disorder; cannabis, cannabis use disorder; CFI, Comparative Fit Index; CPT, Connors Performance Test; CTT2, Color Trails Test II (time); DS, digit span; LNS, letter-number sequencing; OCD, obsessive-compulsive disorder; other drug, other substance use disorder; RMSEA, root mean square error of approximation; SCAP, spatial working memory capacity; SCID, Structured Clinical Interview for DSM-IV-Text Revision; SMAIN, spatial maintenance from the spatial maintenance and manipulation task; SMANIP, spatial maintenance and manipulation task spatial manipulation; SSP, spatial span; SSRT, stop signal reaction time; SZ, schizophrenia; TLI, Tucker-Lewis Index; TS, task-switching; VCAP, verbal working memory capacity; VMAIN, verbal maintenance from the verbal maintenance and manipulation test; VMANIP, verbal maintenance and manipulation test verbal manipulation.

and pons), any significant clusters resulting from whole-brain analyses, and the global structure measures (total GMV, average CT, total SA). We examined relations with each of the brain variables in separate SEMs to reduce collinearity. We also tested an SEM of the direct path of the EF factor to the p factor. For brain variables that were related to both p and EF factors, we tested indirect paths from brain structure to the p factor via the EF factor.

To study the lower-order factors, we used correlated factors measurement models of psychopathology and EF and tested associations between lower-order factors and brain structure variables. We conducted these SEMs in two ways: 1) paths from lower-order factors to each brain structure variable were tested in the same model to partial out their shared variance (thereby, partialing out general p and EF factors); and 2) lower-order factors were separately regressed on brain structure variables (thereby retaining general p and EF factors), as recommended by Forbes *et al.* (53).

SEM analyses were performed in Mplus (version 8.4) (54) using maximum likelihood estimation and bias-corrected bootstrapping procedures with 1000 samples (55). Covariates included gender, age, dummy-coded race/ethnicity, site, and total intracranial volume and average whole-brain FA for analyses of GMV and FA, respectively. We assessed each model's fit to the data using the χ^2 value, Comparative Fit Index, Tucker-Lewis Index, and root mean square error of approximation. Nonsignificant χ^2 tests indicate good model fit; nonetheless, this test generally is overpowered in large samples. Comparative Fit Index and Tucker-Lewis Index > 0.90 indicate adequate fit; root mean square error of approximation < 0.08 is considered acceptable (56). Given the number of tests, we report associations significant at $p < .01\%$ and 99% bias-corrected confidence intervals.

RESULTS

Table 1 shows descriptive statistics for all study variables for the overall sample and each diagnostic group.

Confirmatory Factor Analyses

The models of psychopathology and EF fit the data adequately (Figure 1; Tables S4 and S5). To account for biases within the same response mode (i.e., method effects), the psychopathology CFA included correlations between alcohol, cannabis, and other substance use and a correlation between depression and interpersonal sensitivity. Based on examination of modification indices and residuals, a negative correlation between ADHD and schizophrenia was also added to account for the exclusion criterion that patients with schizophrenia could not also meet ADHD criteria. For the CFA of EF, factor loadings for the Attention Network and Stroop Color-Word Tests were nonsignificant; therefore, they were removed from the analysis.

Exploratory Analyses

Whole-brain VBM analyses revealed that individuals with higher p factor scores had significantly less volume within the right VAC and calcarine cortex (cluster 1) and the left supplementary motor area (SMA) and bilateral anterior cingulate gyrus (cluster 2) (Figure 2A and Table 2). The VAC cluster highly overlapped with the VAC ROI from discovery analyses (18).

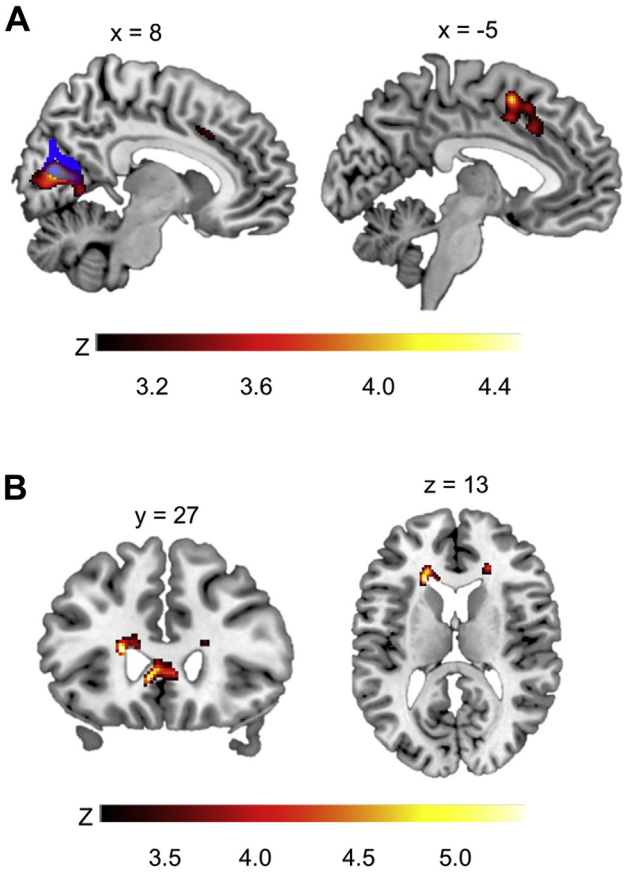

Figure 2. Whole-brain exploratory analyses of differences in gray matter volume and fractional anisotropy related to p factor scores. Statistical parametric maps from exploratory whole-brain analyses are shown to illustrate voxels exhibiting a significant negative correlation with p factor scores controlling for gender, age, dummy-coded race and ethnicity, site, and intracranial volume and average whole-brain fractional anisotropy for the voxel-based morphometry and diffusion tensor imaging analyses, respectively. **(A)** Voxel-based morphometry analyses show gray matter volume reductions in right visual association and calcarine cortices (left panel) and bilateral supplementary motor area and cingulate gyrus (right panel). The mask of the visual association cortex region of interest from the discovery analyses (18) is shown in blue and is overlaid onto the visual association cortex cluster (left panel). **(B)** Diffusion tensor imaging analyses show poorer fractional anisotropy in the bilateral genu of the corpus callosum (left panel) and the bilateral anterior corona radiata (left and right panels). Color bars reflect *z* scores.

Whole-brain DTI analyses revealed significantly decreased FA within bilateral anterior corona radiata (ACR) and genu of the corpus callosum (GCC) (Figure 2B). GMV and FA estimates from these clusters were extracted for SEM analyses (Table S6). The VAC ROI and whole-brain cluster estimates were highly correlated ($r = 0.972$); therefore, we did not subject the whole-brain cluster to further analysis. FA values from the three ACR clusters were averaged.

Direct and Indirect Path Models

Table 3 shows results from SEM analyses testing direct and indirect paths of brain structure to the p factor via the EF factor. In terms of the ROI analyses, higher levels of the

Table 2. Differences in Gray Matter Volume and Fractional Anisotropy Associated With p Factor Scores From Exploratory Whole-Brain Voxel-Based Morphometry and Diffusion Tensor Imaging Analyses

Cluster Size, k	Peak Region	MNI Coordinates			Peak *z* Score	R^2 (p Factor)
		x	y	z		
Voxel-Based Morphometry Analysis						
2555	Right visual association cortex (BA 18)	8	−74	14	4.53	0.074
	Right calcarine cortex	15	−71	15	4.01	0.059
	Right calcarine cortex	14	−59	11	3.86	0.054
975	Left supplementary motor area (BA 6)	−5	8	54	4.08	0.060
	Cingulate gyrus	0	23	39	3.67	0.050
	Left cingulate gyrus, anterior division (BA 32)	−5	6	44	3.58	0.047
Diffusion Tensor Imaging Analysis						
247	Left anterior corona radiata	−21	27	13	4.95	0.087
344	Left genu of corpus callosum (forceps minor)	−8	27	−2	4.83	0.083
	Left genu of corpus callosum (forceps minor)	−17	38	−8	4.17	0.063
	Right genu of corpus callosum (forceps minor)	6	29	3	4.07	0.060
105	Right anterior corona radiata	21	33	13	4.02	0.059
	Right anterior corona radiata	20	26	16	3.51	0.046
97	Right anterior corona radiata	15	44	−8	3.77	0.052
	Right anterior corona radiata	18	38	−0	3.60	0.048
	Right anterior corona radiata	15	33	−6	3.60	0.048

n = 265 for voxel-based morphometry analyses; *n* = 258 for diffusion tensor imaging analyses.
BA, Brodmann area; MNI, Montreal Neurological Institute.

p factor were associated with reduced VAC volume and poorer EF. Higher levels of the EF factor were associated with greater VAC, cerebellar lobule VIIB, and total GMV and greater total SA. The p factor was unrelated to the other ROIs or global structure measures. The EF factor was unrelated to posterior cerebellar GMV, pons FA, and average CT. In terms of the clusters identified from whole-brain analyses, there was a significant direct path from GCC FA to EF; conversely, SMA/cingulate GMV and ACR FA were unrelated to EF.

As VAC GMV and GCC FA were both related to p and EF factors, we tested two indirect path models: 1) VAC GMV → EF → p (Figure 3); and 2) GCC FA → EF → p. In both models, the direct and indirect paths from brain structure to the p factor via the EF factor were significant. At the request of an anonymous reviewer, we included IQ as an additional covariate; results, although attenuated, were robust to the inclusion of IQ (Supplement).

When partialing out the shared variance among the lower-order factors, relations with the brain structure variables were nonsignificant, with the exceptions of significant negative relations between GCC FA and the thought disorders factor and between SMA/cingulate GMV and the internalizing factor (Tables S7 and S8). When separately regressing the lower-order factors on brain structure, VAC GMV was related to internalizing, externalizing, WM, and shifting factors. The general EF factor was related to each of the lower-order psychopathology factors, and the p factor was related to the WM and shifting factors (see Supplemental Results for details).

DISCUSSION

In the CNP sample of 265 healthy adults and patients, we examined direct and indirect associations between brain structure, general psychopathology, and the EF factor. Consistent with our hypotheses, we found direct relations between higher levels of the p factor and decreased levels of the EF factor and VAC GMV, replicating previous studies (18,19). In contrast, we did not replicate previous associations between the p factor and cerebellar GMV, pontine FA (18), global GMV (23,24), or CT (25). New findings from whole-brain analyses revealed reduced SMA/cingulate GMV and ACR and GCC FA in those high in the p factor. Indirect relations between the p factor and VAC and GCC structure via the EF factor also emerged.

Our findings extend prior research showing a relationship between the EF and p factors in a cross-diagnostic case-control sample. Observing an association between the p and EF factors in a sample of patients and healthy adults using comprehensive EF measures is noteworthy because most prior research has been conducted in youth community samples (9–12,14–16) or has focused only on certain EF components (10,13,16). Replication of the negative association between p and VAC GMV in two independent samples also provides continued support for the role of the VAC in general psychopathology. Whole-brain analyses also identified reduced GMV within a VAC cluster that highly overlapped with the VAC discovery ROI (18). Indeed, neuroimaging research has found VAC structural and functional alterations in multiple psychiatric disorders (57–60).

The indirect relation between VAC GMV and the p factor via the EF factor suggests that EF may partially explain the relation between VAC morphology and transdiagnostic psychopathology. The VAC is involved in selection and suppression of incoming relevant versus irrelevant visual information (26–28), a critical component of EF. Consistent with neurocognitive studies indicating visual sensory dysfunction in thought disorders (61,62), a recent study of the CNP sample identified somatosensory-motor dysconnectivity with executive cortical

Table 3. Direct and Indirect Relations of Brain Structure, General Psychopathology, and Executive Function

	p Factor			EF Factor		
Direct Path Models	Std Estimate	SE	99% Bias-Corrected CI	Std Estimate	SE	99% Bias-Corrected CI
ROIs						
EF Factor	−0.340[a]	0.070	(−0.486 to −0.164)			
VAC GMV	−0.270[a]	0.083	(−0.488 to −0.059)	0.184[a]	0.059	(0.029 to 0.346)
Cerebellar GMV	0.013	0.074	(−0.177 to 0.205)	0.128	0.063	(−0.021 to 0.281)
Lobule VIIB GMV	0.041	0.073	(−0.160 to 0.221)	0.211[a]	0.059	(0.051 to 0.359)
Pons FA	−0.008	0.073	(−0.177 to 0.187)	0.073	0.054	(−0.070 to 0.202)
Exploratory Clusters						
SMA/Cingulate GMV				0.068	0.067	(−0.094 to 0.240)
ACR FA				0.122	0.071	(−0.071 to 0.295)
GCC FA				0.276[a]	0.068	(0.090 to 0.448)
Global Structure						
Total GMV	−0.186	0.097	(−0.419 to 0.067)	0.255[a]	0.071	(0.068 to 0.422)
Average CT	−0.076	0.070	(−0.261 to 0.106)	−0.013	0.065	(−0.178 to 0.140)
Total SA	−0.161	0.086	(−0.389 to 0.064)	0.213[a]	0.061	(0.055 to 0.361)

Indirect Path Models	Std. Estimate	SE	99% Bias-Corrected CI
IE: VAC GMV→EF→p	−0.062[a]	0.027	(−0.174 to −0.015)
DE: VAC GMV→p	−0.197[a]	0.077	(−0.390 to −0.005)
IE: GCC FA→EF→p	−0.065[a]	0.028	(−0.165 to −0.013)
DE: GCC FA→p	−0.409[a]	0.070	(−0.568 to −0.223)

Direct and indirect path models are shown. The direct path models include the path from the EF factor to the p factor, paths from the four ROIs to the p and EF factors, paths from the three regions identified from exploratory analyses to the p and EF factors, and paths from the three global structure measures (total GMV, average CT, total SA) to the p and EF factors in 20 separate models. Covariates included gender, age, dummy-coded race and ethnicity, site, and total intracranial volume or average whole-brain FA, for analyses of GMV or FA, respectively (not shown for brevity). Two indirect path models also are shown: 1) VAC GMV to the p factor via the EF factor; and 2) GCC FA to the p factor via the EF factor. Within each of these indirect path models, the direct path from brain structure to the p factor via the EF factor also is shown (i.e., Path C′ in Figure 3 for indirect path model of VAC GMV). Standardized estimates and bias-corrected 99% CIs are shown. n = 265 for all models of GMV; n = 258 for all models of FA except for models of pons FA, for which n = 223.

ACR, anterior corona radiata; CT, cortical thickness; DE, direct effect; EF, executive function; FA, fractional anisotropy; GCC, genu of the corpus callosum; GMV, gray matter volume; IE, indirect effect; ROIs, regions of interest; SA, surface area; SMA, supplementary motor area; Std., standardized; VAC, visual association cortex; →, "predicting."

[a]Estimates significant at $p < .01$.

networks related to general psychopathology, cognitive dysfunction, and impulsivity (63). Functional connectivity between VAC and frontoparietal and default mode networks, involved in executive control and self-referential processing, respectively, also has been related to the p factor (33). This suggests that VAC structural alterations may reflect impairments in the integration of bottom-up sensory information with top-down executive control and attentional processes, which may be executive dysfunctions present across diagnostic boundaries.

It is also likely that other factors explain the relation between VAC structure and the p factor. For example, the VAC is also involved in associative memory formation (64), a critical component of episodic memory, dysfunctions of which also are present in multiple disorders (65). In addition, it may be important to consider the role of early-life experiences on the development of EF processes supported by the VAC. In this context, Rosen, *et al.* (66) posited that differences in socioeconomic status and early cognitive stimulation impact the development of VAC-prefrontal cortex circuitry and subsequent EF skills. Future research should examine relations between VAC-prefrontal cortex circuit structure/function, the EF factor, and the p factor across development.

Exploratory analyses revealed that individuals with high levels of the p factor had less volume within the SMA extending into the dorsal anterior cingulate cortex. This finding is consistent with transdiagnostic meta-analyses that identified common structural alterations in dorsal anterior cingulate (67) and abnormal activation of midcingulate and pre-SMA during cognitive control tasks (68) in five psychiatric disorders. Whole-brain analyses also showed that those with high levels of the p factor demonstrated poorer ACR and GCC white matter integrity. The ACR are projection fibers that reciprocally connect the thalamus and cerebral cortex as part of a limbic-thalamocortical circuitry (69) and are involved in executive attentional control and conflict resolution (70,71). The GCC are commissural fibers connecting prefrontal cortical hemispheres involved in cognitive function (72). Both reduced ACR and reduced GCC FA have been identified in multiple psychiatric disorders (70,73,74), and poorer GCC FA has been associated with a higher p factor (75). We found an indirect relation between GCC FA and the p factor via the EF factor, suggesting that high p factor individuals show relatively poorer communication between prefrontal cortical regions, which may be manifested by individual differences in the EF factor. As these findings were exploratory, future studies should test their replicability.

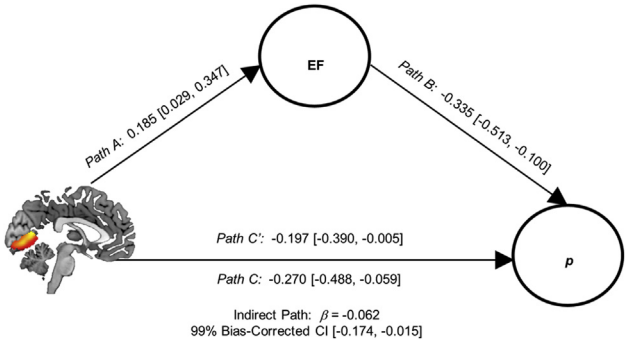

Figure 3. Indirect relation of visual association cortex gray matter volume and general psychopathology through executive function (EF). The indirect path analysis of visual association cortex (VAC) gray matter volume (GMV) predicting the p factor via the EF factor is shown. Direct paths from VAC GMV to the EF (Path A) and p factors (Path C) and from the EF factor to the p factor (Path B) are shown. The indirect path of VAC GMV to the p factor via EF was significant. The direct path from VAC GMV to the p factor remains significant with the inclusion of the EF factor in the model (Path C′). Standardized weights and 99% bias-corrected confidence intervals (CIs) are shown. Paths from gender, age, dummy-coded ethnicity and race, site, and total intracranial volume to VAC GMV and p and EF factors are not shown.

Interestingly, when partialing out the shared variance of the lower-order factors in the p and EF factors, relations between brain structure and lower-order psychopathology and EF factors were nonsignificant, with few exceptions. GCC FA was uniquely negatively related to thought disorders, which is supported by a meta-analysis showing reduced GCC FA in patients with schizophrenia (73). When examining the lower-order factors independently (thereby retaining their full variance), general EF was related to all three lower-order psychopathology factors, and the p factor was related to WM and shifting factors, suggesting a general, nonspecific relation between EF and psychopathology, consistent with previous research (9,12). Overall, these findings suggest that the relationships between brain structure, the p factor, and the EF factor are generalizable across families of disorders and EF components. This is consistent with research demonstrating little to no unique relations between CT and internalizing, externalizing, and thought disorder factors apart from the p factor in adults (25).

There are many differences between previous studies identifying relations between the p factor and CTCC and global brain structure and the current study that may have contributed to lack of replication. Moderators of replicability include the type of sample (community/volunteer vs. case-control), representativeness of certain disorders over others (entire symptom spectrum vs. primarily schizophrenia, bipolar, and ADHD symptoms), and power to detect effects. Differences in sample age also may have led to the discrepancy in results. Studies reporting an association between CTCC morphology and transdiagnostic psychopathology have been conducted in adolescents (20) or young adults (18). In contrast, samples in which nonreplication was found included individuals in midlife (19) or young adulthood to midlife as in the current study. This raises the possibility that CTCC structure associations with the p factor may reflect different influences of brain structure on risk across development. The contribution of CTCC structure to p may be greater earlier than later in life, which may reflect the still-active structural development of the cerebellum (76). Longitudinal assessments of brain structure and the p factor are necessary to evaluate possible developmental differences.

Our study has several limitations. First, as it is cross-sectional, we cannot establish temporal order among the observed links between brain structure, the EF factor, and the p factor; therefore, we are careful to interpret SEM paths as correlational, not causal. Future longitudinal research should examine this question. Second, the CNP study inclusion criteria specified that each patient group could not meet criteria for either of the other two disorders. This recruitment strategy precluded some of the natural comorbidity between these disorders, thereby limiting the amount of overlap that could be identified by the p factor. Thus, the p factor identified in this study may not have the same meaning as in community samples. Third, different mental health measures were administered to the healthy versus patient groups, with only a few measures administered to everyone, limiting symptom assessment across groups. Despite these limitations, a p factor still was identifiable, and 81% of patients met criteria for more than one disorder. However, our failure to replicate associations between CTCC structure and the p factor may be partially due to these limitations. Fourth, after visual inspection of the FA maps, 34 participants (~13%) did not have adequate pons coverage, which limited our power to detect significant associations between pons FA and the p factor and EF factors. Fifth, given the high rates of psychotropic medication use by patients (73%), we could not separate the effect of the p factor from the effect of medication use on brain structure and EF.

Despite these limitations, our results support the hypothesis that executive dysfunction is a transdiagnostic correlate of general psychopathology. The replicable associations of the p factor with VAC GMV in the current study and in two other very different independent samples (18,19) provide strong evidence for the role of VAC structural alterations in general psychopathology. Moreover, our results suggest that executive dysfunction may partially explain associations between VAC structure and general psychopathology. Exploratory analyses also identified novel targets for future research within the SMA/cingulate cortex, ACR, and GCC. These findings may point to transdiagnostic intervention approaches that could target specific cognitive processes supported by the VAC. For example, interventions targeting attentional and memory biases in the selection and retention of task-relevant information may lead to improved symptoms spanning diagnostic categories. Further, brain-based interventions (e.g., transcranial direct-current stimulation) targeting prefrontal-VAC circuitry could improve transdiagnostic symptoms. However, longitudinal neuroimaging research is needed to better determine the clinical implications of this research.

ACKNOWLEDGMENTS AND DISCLOSURES

This work was partially supported by grants from the National Institutes of Health (Grant Nos. R01 MH101521 and R37 MH068376 [to DAP]) and the Ruth L. Kirschstein National Research Service Award (Grant No. F32 MH124409 [to ALR]). The Consortium for Neuropsychiatric Phenomics (CNP) study was supported by the Consortium for Neuropsychiatric Phenomics (National Institutes of Health Roadmap for Medical Research grants)

(Grant No. UL1-DE019580; principal investigator, Robert M. Bilder). The content is solely the responsibility of the authors and does not necessarily represent the official views of the National Institutes of Health or the Consortium for Neuropsychiatric Phenomics investigators.

We thank the investigators Robert Bilder, Russell Poldrack, Tyrone Cannon, Edythe London, Nelson Freimer, Eliza Congdon, Katherine Karlsgodt, and Fred Sabb for sharing their data publicly. In particular, the authors would like to acknowledge Dr. Robert Bilder (University of California, Los Angeles) for his generous assistance with the dataset. We also would like to acknowledge Monica Landi, M.S.W., and Rachel Lobien, B.A., from the Center for Depression, Anxiety and Stress Research at McLean Hospital for their assistance with clinical data entry.

All data are publicly available via the OpenfMRI database (https://openfmri.org/dataset/). The accession number of this study is ds000030.

Over the past 3 years, DAP has received consulting fees from BlackThorn Therapeutics, Boehringer Ingelheim, Compass Pathway, Concert Pharmaceuticals, Engrail Pharmaceuticals, Otsuka Pharmaceuticals, and Takeda Pharmaceuticals; an honorarium from Alkermes; and research funding from the National Institute of Mental Health, Dana Foundation, Brain and Behavior Research Foundation, Millennium Pharmaceuticals. In addition, he has received stock options from BlackThorn Therapeutics. No funding from these entities was used to support the current work, and all views expressed are solely those of the authors. ALR reports no biomedical financial interests or potential conflicts of interest.

ARTICLE INFORMATION

From the Center for Depression, Anxiety and Stress Research (ALR, DAP) and McLean Imaging Center (DAP), McLean Hospital; and Harvard Medical School (ALR, DAP), Belmont, Massachusetts.

Address correspondence to Adrienne L. Romer, Ph.D., at aromer@mclean.harvard.edu.

Received Feb 12, 2021; revised May 20, 2021; accepted Jun 3, 2021.

Supplementary material cited in this article is available online at https://doi.org/10.1016/j.bpsgos.2021.06.002.

REFERENCES

1. Kessler RC, Chiu WT, Demler O, Merikangas KR, Walters EE (2005): Prevalence, severity, and comorbidity of 12-month DSM-IV disorders in the National Comorbidity Survey replication. Arch Gen Psychiatry 62:617–627.
2. Caspi A, Moffitt TE (2018): All for one and one for all: Mental disorders in one dimension. Am J Psychiatry 175:831–844.
3. Lahey BB, Krueger RF, Rathouz PJ, Waldman ID, Zald DH (2017): A hierarchical causal taxonomy of psychopathology across the life span. Psychol Bull 143:142–186.
4. Caspi A, Houts RM, Ambler A, Danese A, Elliott ML, Hariri A, *et al.* (2020): Longitudinal assessment of mental health disorders and comorbidities across 4 decades among participants in the Dunedin Birth Cohort Study. JAMA Netw Open 3:e203221.
5. Snyder HR, Miyake A, Hankin BL (2015): Advancing understanding of executive function impairments and psychopathology: Bridging the gap between clinical and cognitive approaches. Front Psychol 6:328.
6. McTeague LM, Goodkind MS, Etkin A (2016): Transdiagnostic impairment of cognitive control in mental illness. J Psychiatr Res 83:37–46.
7. Abramovitch A, Short T, Schweiger A (2021): The c factor: Cognitive dysfunction as a transdiagnostic dimension in psychopathology. Clin Psychol Rev 86:102007.
8. Zelazo PD (2020): Executive function and psychopathology: A neurodevelopmental perspective. Annu Rev Clin Psychol 16:431–454.
9. Bloemen AJP, Oldehinkel AJ, Laceulle OM, Ormel J, Rommelse NNJ, Hartman CA (2018): The association between executive functioning and psychopathology: General or specific? Psychol Med 48:1787–1794.
10. Huang-Pollock C, Shapiro Z, Galloway-Long H, Weigard A (2017): Is poor working memory a transdiagnostic risk factor for psychopathology? J Abnorm Child Psychol 45:1477–1490.
11. Martel MM, Pan PM, Hoffmann MS, Gadelha A, do Rosário MC, Mari JJ, *et al.* (2017): A general psychopathology factor (P factor) in children: Structural model analysis and external validation through familial risk and child global executive function. J Abnorm Psychol 126:137–148.
12. White LK, Moore TM, Calkins ME, Wolf DH, Satterthwaite TD, Leibenluft E, *et al.* (2017): An evaluation of the specificity of executive function impairment in developmental psychopathology. J Am Acad Child Adolesc Psychiatry 56:975–982.e3.
13. Caspi A, Houts RM, Belsky DW, Goldman-Mellor SJ, Harrington H, Israel S, *et al.* (2014): The p factor: One general psychopathology factor in the structure of psychiatric disorders? Clin Psychol Sci 2:119–137.
14. Wade M, Zeanah CH, Fox NA, Nelson CA (2020): Global deficits in executive functioning are transdiagnostic mediators between severe childhood neglect and psychopathology in adolescence. Psychol Med 50:1687–1694.
15. Snyder HR, Friedman NP, Hankin BL (2019): Transdiagnostic mechanisms of psychopathology in youth: Executive functions, dependent stress, and rumination. Cognit Ther Res 43:834–851.
16. Castellanos-Ryan N, Brière FN, O'Leary-Barrett M, Banaschewski T, Bokde A, Bromberg U, *et al.* (2016): The structure of psychopathology in adolescence and its common personality and cognitive correlates. J Abnorm Psychol 125:1039–1052.
17. Cardenas-Iniguez C, Moore TM, Kaczkurkin AN, Meyer FAC, Satterthwaite TD, Fair DA, *et al.* (2020): Direct and indirect associations of widespread individual differences in brain white matter microstructure with executive functioning and general and specific dimensions of psychopathology in children [published online ahead of print Nov 25]. Biol Psychiatry Cogn Neurosci Neuroimaging.
18. Romer AL, Knodt AR, Houts R, Brigidi BD, Moffitt TE, Caspi A, Hariri AR (2018): Structural alterations within cerebellar circuitry are associated with general liability for common mental disorders. Mol Psychiatry 23:1084–1090.
19. Romer AL, Knodt AR, Sison ML, Ireland D, Houts R, Ramrakha S, *et al.* (2021): Replicability of structural brain alterations associated with general psychopathology: Evidence from a population-representative birth cohort. Mol Psychiatry 26:3839–3846.
20. Moberget T, Alnæs D, Kaufmann T, Doan NT, Córdova-Palomera A, Norbom LB, *et al.* (2019): Cerebellar gray matter volume is associated with cognitive function and psychopathology in adolescence. Biol Psychiatry 86:65–75.
21. Middleton FA, Strick PL (2001): Cerebellar projections to the prefrontal cortex of the primate. J Neurosci 21:700–712.
22. Buckner RL (2013): The cerebellum and cognitive function: 25 years of insight from anatomy and neuroimaging. Neuron 80:807–815.
23. Kaczkurkin AN, Park SS, Sotiras A, Moore TM, Calkins ME, Cieslak M, *et al.* (2019): Evidence for dissociable linkage of dimensions of psychopathology to brain structure in youths. Am J Psychiatry 176:1000–1009.
24. Durham EL, Jeong HJ, Moore TM, Dupont RM, Cardenas-Iniguez C, Cui Z, *et al.* (2021): Association of gray matter volumes with general and specific dimensions of psychopathology in children. Neuropsychopharmacology 46:1333–1339.
25. Romer AL, Elliott ML, Knodt AR, Sison ML, Ireland D, Houts R, *et al.* (2021): Pervasively thinner neocortex as a transdiagnostic feature of general psychopathology. Am J Psychiatry 178:174–182.
26. Chadick JZ, Gazzaley A (2011): Differential coupling of visual cortex with default or frontal-parietal network based on goals. Nat Neurosci 14:830–832.
27. Gazzaley A, Rissman J, Cooney J, Rutman A, Seibert T, Clapp W, D'Esposito M (2007): Functional interactions between prefrontal and visual association cortex contribute to top-down modulation of visual processing. Cereb Cortex 17(suppl 1):i125–i135.
28. Karten A, Pantazatos SP, Khalil D, Zhang X, Hirsch J (2013): Dynamic coupling between the lateral occipital-cortex, default-mode, and

frontoparietal networks during bistable perception. Brain Connect 3:286–293.
29. Krienen FM, Buckner RL (2009): Segregated fronto-cerebellar circuits revealed by intrinsic functional connectivity. Cereb Cortex 19:2485–2497.
30. Le TM, Borghi JA, Kujawa AJ, Klein DN, Leung HC (2017): Alterations in visual cortical activation and connectivity with prefrontal cortex during working memory updating in major depressive disorder. NeuroImage Clin 14:43–53.
31. Stoodley CJ, Schmahmann JD (2009): Functional topography in the human cerebellum: A meta-analysis of neuroimaging studies. Neuroimage 44:489–501.
32. E KH, Chen SH, Ho MH, Desmond JE (2014): A meta-analysis of cerebellar contributions to higher cognition from PET and fMRI studies. Hum Brain Mapp 35:593–615.
33. Elliott ML, Romer A, Knodt AR, Hariri AR (2018): A connectome-wide functional signature of transdiagnostic risk for mental illness. Biol Psychiatry 84:452–459.
34. Ito M (1993): Movement and thought: Identical control mechanisms by the cerebellum. Trends Neurosci 16:448–450; discussion 453–454.
35. Ito M (2008): Control of mental activities by internal models in the cerebellum. Nat Rev Neurosci 9:304–313.
36. Bernard JA, Mittal VA (2015): Dysfunctional activation of the cerebellum in schizophrenia: A functional neuroimaging meta-analysis. Clin Psychol Sci 3:545–566.
37. Cao H, Chén OY, Chung Y, Forsyth JK, McEwen SC, Gee DG, *et al.* (2018): Cerebello-thalamo-cortical hyperconnectivity as a state-independent functional neural signature for psychosis prediction and characterization. Nat Commun 9:3836.
38. Moberget T, Doan NT, Alnæs D, Kaufmann T, Córdova-Palomera A, Lagerberg TV, *et al.* (2018): Cerebellar volume and cerebellocerebral structural covariance in schizophrenia: A multisite mega-analysis of 983 patients and 1349 healthy controls. Mol Psychiatry 23:1512–1520.
39. Andreasen NC, Paradiso S, O'Leary DS (1998): "Cognitive Dysmetria" as an integrative theory of schizophrenia: A dysfunction in cortical-subcortical-cerebellar circuitry? Schizophr Bull 24:203–218.
40. Schmahmann JD (2004): Disorders of the cerebellum: Ataxia, dysmetria of thought, and the cerebellar cognitive affective syndrome. J Neuropsychiatry Clin Neurosci 16:367–378.
41. Schmahmann JD, Weilburg JB, Sherman JC (2007): The neuropsychiatry of the cerebellum - Insights from the clinic. Cerebellum 6:254–267.
42. Poldrack RA, Congdon E, Triplett W, Gorgolewski KJ, Karlsgodt KH, Mumford JA, *et al.* (2016): A phenome-wide examination of neural and cognitive function. Sci Data 3:160110.
43. Poldrack RA, Gorgolewski KJ (2017): OpenfMRI: Open sharing of task fMRI data. Neuroimage 144:259–261.
44. First MB, Spitzer RL, Gibbon M, Williams JBW (2002): Structured Clinical Interview for DSM-IV-TR Axis I Disorders, Research Version, Patient Edition. New York: New York State Psychiatric Institute.
45. Miyake A, Friedman NP, Emerson MJ, Witzki AH, Howerter A, Wager TD (2000): The unity and diversity of executive functions and their contributions to complex "frontal lobe" tasks: A latent variable analysis. Cogn Psychol 41:49–100.
46. Ashburner J, Friston KJ (2005): Unified segmentation. Neuroimage 26:839–851.
47. Ashburner J (2007): A fast diffeomorphic image registration algorithm. Neuroimage 38:95–113.
48. Diedrichsen J, Balsters JH, Flavell J, Cussans E, Ramnani N (2009): A probabilistic MR atlas of the human cerebellum. Neuroimage 46:39–46.
49. Gorgolewski KJ, Durnez J, Poldrack RA (2017): Preprocessed Consortium for Neuropsychiatric Phenomics dataset. F1000Res 6:1262.
50. Dale AM, Fischl B, Sereno MI (1999): Cortical surface-based analysis. I. Segmentation and surface reconstruction. Neuroimage 9:179–194.
51. Bonifay W, Lane SP, Reise SP (2017): Three concerns with applying a bifactor model as a structure of psychopathology. Clin Psychol Sci 5:184–186.
52. Kotov R, Krueger RF, Watson D, Achenbach TM, Althoff RR, Bagby RM, *et al.* (2017): The Hierarchical Taxonomy of Psychopathology (HiTOP): A dimensional alternative to traditional nosologies. J Abnorm Psychol 126:454–477.
53. Forbes MK, Greene AL, Levin-Aspenson HF, Watts AL, Hallquist M, Lahey BB, *et al.* (2021): Three recommendations based on a comparison of the reliability and validity of the predominant models used in research on the empirical structure of psychopathology. J Abnorm Psychol 130:297–317.
54. Muthen LK, Muthen BO (1998): Mplus User's Guide, 8th ed. Los Angeles: Muthen & Muthen.
55. MacKinnon DP, Lockwood CM, Williams J (2004): Confidence limits for the indirect effect: Distribution of the product and resampling methods. Multivariate Behav Res 39:99.
56. Kline RB (2015): Principles and Practice of Structural Equation Modeling, 4th ed. New York: Guilford Publications.
57. Yang X, Ma X, Huang B, Sun G, Zhao L, Lin D, *et al.* (2015): Gray matter volume abnormalities were associated with sustained attention in unmedicated major depression. Compr Psychiatry 63:71–79.
58. Horn H, Federspiel A, Wirth M, Müller TJ, Wiest R, Walther S, Strik W (2010): Gray matter volume differences specific to formal thought disorder in schizophrenia. Psychiatry Res 182:183–186.
59. Jung J, Kang J, Won E, Nam K, Lee MS, Tae WS, Ham BJ (2014): Impact of lingual gyrus volume on antidepressant response and neurocognitive functions in major depressive disorder: A voxel-based morphometry study. J Affect Disord 169:179–187.
60. Borgwardt SJ, Picchioni MM, Ettinger U, Toulopoulou T, Murray R, McGuire PK (2010): Regional gray matter volume in monozygotic twins concordant and discordant for schizophrenia. Biol Psychiatry 67:956–964.
61. Javitt DC, Freedman R (2015): Sensory processing dysfunction in the personal experience and neuronal machinery of schizophrenia. Am J Psychiatry 172:17–31.
62. Mrad A, Wassim Krir M, Ajmi I, Gaha L, Mechri A (2016): Neurological soft signs in euthymic bipolar I patients: A comparative study with healthy siblings and controls. Psychiatry Res 236:173–178.
63. Kebets V, Holmes AJ, Orban C, Tang S, Li J, Sun N, *et al.* (2019): Somatosensory-motor dysconnectivity spans multiple transdiagnostic dimensions of psychopathology. Biol Psychiatry 86:779–791.
64. Rosen ML, Sheridan MA, Sambrook KA, Peverill MR, Meltzoff AN, McLaughlin KA (2018): The role of visual association cortex in associative memory formation across development. J Cogn Neurosci 30:365–380.
65. Barry T, Hallford DJ, Takano K (2020): Autobiographical memory impairments as a transdiagnostic feature of mental illness: A meta-analysis of autobiographical memory specificity and overgenerality amongst people with psychiatric diagnoses. PsyArXiv. https://doi.org/10.31234/osf.io/ab5cu.
66. Rosen ML, Amso D, McLaughlin KA (2019): The role of the visual association cortex in scaffolding prefrontal cortex development: A novel mechanism linking socioeconomic status and executive function. Dev Cogn Neurosci 39:100699.
67. Goodkind M, Eickhoff SB, Oathes DJ, Jiang Y, Chang A, Jones-Hagata LB, *et al.* (2015): Identification of a common neurobiological substrate for mental illness. JAMA Psychiatry 72:305–315.
68. McTeague LM, Huemer J, Carreon DM, Jiang Y, Eickhoff SB, Etkin A (2017): Identification of common neural circuit disruptions in cognitive control across psychiatric disorders. Am J Psychiatry 174:676–685.
69. Mori S, Oishi K, Jiang H, Jiang L, Li X, Akhter K, *et al.* (2008): Stereotaxic white matter atlas based on diffusion tensor imaging in an ICBM template. Neuroimage 40:570–582.

70. Choi S, Han KM, Won E, Yoon BJ, Lee MS, Ham BJ (2015): Association of brain-derived neurotrophic factor DNA methylation and reduced white matter integrity in the anterior corona radiata in major depression. J Affect Disord 172:74–80.
71. Yin X, Han Y, Ge H, Xu W, Huang R, Zhang D, *et al.* (2013): Inferior frontal white matter asymmetry correlates with executive control of attention. Hum Brain Mapp 34:796–813.
72. Luders E, Narr KL, Bilder RM, Thompson PM, Szeszko PR, Hamilton L, Toga AW (2007): Positive correlations between corpus callosum thickness and intelligence. Neuroimage 37:1457–1464.
73. Kelly S, Jahanshad N, Zalesky A, Kochunov P, Agartz I, Alloza C, *et al.* (2018): Widespread white matter microstructural differences in schizophrenia across 4322 individuals: Results from the ENIGMA Schizophrenia DTI Working Group. Mol Psychiatry 23:1261–1269.
74. Thomason ME, Thompson PM (2011): Diffusion imaging, white matter, and psychopathology. Annu Rev Clin Psychol 7:63–85.
75. Riem MME, van Hoof MJ, Garrett AS, Rombouts SARB, van der Wee NJA, van IJzendoorn MH, Vermeiren RRJM (2019): General psychopathology factor and unresolved-disorganized attachment uniquely correlated to white matter integrity using diffusion tensor imaging. Behav Brain Res 359:1–8.
76. Diamond A (2000): Close interrelation of motor development and cognitive development and of the cerebellum and prefrontal cortex. Child Dev 71:44–56.